

Chemometric-assisted fingerprinting profiling of the Pagoda (*Clerodendrum paniculatum* L.) extract variation using proton nuclear magnetic resonance (¹H NMR) method, compound isolation, and cytotoxic activity

Budiman YASIR^{1,2} , Muh AZWAR AR^{1,2} , Andi PALUSERI^{1,2} , Muhammad Akmal SUKARA³ , Yohei SAITO⁴ , Kyoko NAKAGAWA-GOTO⁴ , Muhammad RAIHAN⁵ , Gemini ALAM⁵ , Abdul ROHMAN^{6*} 

¹ Almarisah Madani University, Faculty of Health Sciences, Makassar, 90245, Indonesia

² Sekolah Tinggi Ilmu Farmasi Makassar, Makassar, 90242, Indonesia

³ Megarezky University, Faculty of Pharmacy, Makassar, 90245, Indonesia

⁴ Kanazawa University, School of Pharmaceutical Sciences, College of Medical, Pharmaceutical and Health Sciences, Kanazawa, 920-1192, Japan

⁵ Hasanuddin University, Department of Pharmacognosy-Phytochemistry Laboratory, Faculty of Pharmacy, Makassar, 90245, Indonesia

⁶ Gadjah Mada University, Department of Pharmaceutical Analysis and Medicinal Chemistry, Faculty of Pharmacy, Yogyakarta, 55281, Indonesia

* Corresponding Author. E-mail: abdulkimfar@gmail.com (A.R.); Tel. +62-878-3844 52 16.

Received: 16 February 2024 / Revised: 27 July 2024 / Accepted: 29 July 2024

ABSTRACT: One of the best solutions to understanding the chemical data of complex natural substances is to use chemometric techniques. This research aims to apply chemometric techniques, specifically principal component analysis (PCA) and cluster analysis (CA), to determine the fingerprint profiles of nine pagoda extracts (PCP) and their isolated compounds using ¹H NMR data and to conduct initial cytotoxicity tests on the extracts. PCP flowers were extracted using various solvents and extraction methods, resulting in 9 types of extracts. The methanol-extracted flower portion was subjected to maceration and the compounds were then isolated using various techniques, including silica gel, column chromatography, and preparative thin layer chromatography (PTLC), which yielded 3 types of compounds. The structures were identified using 1D and 2D NMR and mass spectrometry. Meanwhile, their cytotoxic activity was tested on MCF-7, A549, KB, KB-VIN, and MDA-MB-231 cancer cells using the sulforhodamine B (SRB) assay. The research results revealed that compounds (1) stigmasta-5,22,25-trien-3 β -ol, (2) 6-nonadecenoic acid, and (3) 6,9-nonadecadienoic acid, methyl ester was discovered in this plant for the first time. The fingerprinting profile of the PCP extracts and compounds showed resonance at δ_H 5.33 ppm (*m*, 1H) and δ_H 5.24 ppm (*m*, 1H). PCA of the 12 samples with eigenvalues > 1 explained 91% of the data and exhibited a normal distribution. The score plot was influenced by PC1 (82.2%) and PC2 (10.5%). The loading plot and CA combined with the linearity of (1), (2), and (3) with respect to the variation in extracts had determination coefficients ($R^2 = 0.7550 - 0.9288$) and similarities (78.26% - 98.98%). Cytotoxicity activity showed weak growth inhibition (> 89.6%) in all tested cancer cell types. In conclusion, ¹H NMR spectrum and chemometrics detects the fingerprinting profile of Pagoda extract variations, clustering extracts, identifying marker compounds, and potential for cytotoxicity studies in cancer cells.

KEYWORDS: Chemometrics; *Clerodendrum paniculatum*, spectroscopy, cytotoxicity

1. INTRODUCTION

Pagoda, also known as *Clerodendrum paniculatum* (PCP), is a plant within the *Clerodendrum* genus, which belongs to the *Verbenaceae* or *Lamiaceae* family consisting of over 500 species [2, 3]. This plant thrives in tropical and subtropical regions and grows as a small tree, shrub, or herb [1]. The plants under the genus of *Clerodendrum* have been reported for exhibits various bioactivities, including cytotoxic, antiproliferative, antibacterial, antiparasitic, and anti-inflammatory properties [2]. It also demonstrates antinociceptive, antioxidant, antihypertensive, anticancer, antimicrobial, antidiarrheal, hepatoprotective, hypoglycemic, hypolipidemic, memory-enhancing, and neuroprotective effects [3].

How to cite this article: Yasir B, Azwar Ar M, Paluseri A, Sukara MA, Saito Y, Nakagawa-Goto K, Raihan M, Alam G, Rohman A. Chemometric-assisted fingerprinting profiling of the Pagoda (*Clerodendrum paniculatum* L.) extract variation using proton nuclear magnetic resonance (¹H NMR) method, compound isolation, and cytotoxic activity. J Res Pharm. 2025; 29(3): 971-984.

Several reports showed that PCP offers ranges of pharmacological activities and it has been observed through the studies of various plant parts and solvent extractions. For instance, ethanol extracts from the leaves have demonstrated potential efficacy against SARS-CoV-2 [5, 12]. Ethanol extracts from flowers was investigated and reported to exhibit antidiabetic and antilipidemic activities [6]. Ethyl acetate extract from leaves and ethanol extract from flowers showed antioxidant and hepatoprotective properties [7, 8]. Ethyl acetate extract from the aerial parts were reported for the anticonvulsant properties [4], whereas ethyl acetate fraction from the leaves have shown inhibitory effects against *Pseudomonas aeruginosa* [9]. A study on the hexane extract from the flowers indicated the cytotoxic effects of this plant [1]. A more specific compound known as clerodol from leaves acts as a coronavirus protease inhibitor [10]. Furthermore, ethyl acetate extract from the leaves was reported for its antimicrobial properties, while methanolic extract indicated a potential radical scavenging activity [11].

These pharmacological activities associated with PCP are a result of the presence of several metabolites and compounds that are highly correlated with these activities [13]. Recent advancements in untargeted and targeted fingerprinting methods involve the use of various chromatographic and spectroscopic tools to analyze compounds in the plant extracts [14]. Analytical instruments, such as GC-MS for PCP flower parts, have successfully identified compounds such as pilocarpine, glyceric acid, pangamic acid, and gallic acid. Moreover, HPTLC has been employed to detect quercetin [7]. LC-MS analysis has demonstrated that the ethanol extract of PCP leaves contains compounds such as erucamide, caffeic acid, 7-hydroxycoumarin, and linamarin, whereas the ethyl acetate fraction includes erucamide, apigenin, caffeic acid, kynurenic acid, apigenin 7-O-glucuronide, 6-O-methyl scutellarin, apigetrin, 4-methoxycinnamic acid, 4-coumaric acid, scutellarin, and 7-hydroxycoumarin [9]. TLC has indicated the presence of terpenoids, flavonoids, alkaloids, and tannins in hexane, ethanol, and methanol extracts from various parts of the plant (flower, stem, and leaf) [1]. An important triterpenoid, clerodol, has been identified in the leaves of PCP [10]. GC-HRMS analysis of the hexane extract from the leaves predicted the presence of major compounds such as phytol, 22-tritetracontanone, 6,9,12-octadecatrienoic acid, and phenyl methyl ester, whereas the ethyl acetate extract was predicted to contain phytol. Furthermore, LC-HRMS analysis of the methanolic extract revealed significant fractions, including 8', 10' dihydroxydihydroergotamine, khayanthone, galactonic acid, calotropin, and 26,26,26,27,27,27-hexafluoro-1 α ,24-dihydroxy vitamin D3 [11]. Finally, LC-MS/MS analysis of the alcohol extract from the leaves confirmed the presence of compounds such as komarovicine and roemerine [12].

The use of proton nuclear magnetic resonance ($^1\text{H-NMR}$) chemical shift fingerprinting across diverse regions offers valuable insights into the identification, detection of adulteration, and quality control of herbal plants [15, 18]. This method is known for its simplicity, robustness, and reproducibility in metabolomic profiling based on $^1\text{H-NMR}$ spectroscopy for various plant extract applications [17]. The application of $^1\text{H-NMR}$ analysis, when coupled with chemometrics techniques such as principal component analysis (PCA) and cluster analysis (CA), is important for categorizing chemical constituents, assessing similarities, and discerning the metabolomic fingerprint profiles of herbal plants [15, 16, 18]. Despite an extensive review of the literature, there is currently no comprehensive study addressing the fingerprint profiles of different PCP flower extract variations using various solvents (methanol, ethanol, and hexane) and extraction methods (maceration, MAE, and reflux) along with $^1\text{H-NMR}$ spectroscopy and chemometric methods (PCA and CA).

In the background of this research, there is a need to develop more sophisticated and efficient analytical methods to understand the variation of secondary metabolites from herbal plants such as Pagoda. Secondary metabolites in plants have long been known to have significant pharmacological potential, but identifying and deeply understanding these compounds are often complex and time-consuming. Therefore, the novelty of this research aims to present an innovative approach by utilizing NMR spectroscopy techniques ($^1\text{H NMR}$) with solvent variations and extraction methods, as well as chemometric analysis, to generate fingerprinting profiles of extracts and isolate key compounds. This approach is expected to provide deeper insights into the variation of chemical compounds in Pagoda, facilitate the identification of compounds with significant biological activities, and provide a foundation for the development of more effective and efficient plant-based drugs. Thus, this research is expected to be an important initial step in accelerating the discovery and utilization of the therapeutic potential of these medicinal plants. This research aims to obtain fingerprint profiles of extracts and isolate compounds and preliminarily evaluate the cytotoxic activity of these extracts against various cancer cell cultures.

2. RESULTS AND DISCUSSION

2.1. Fingerprint profiling of pagoda extracts

In this study, 12 different samples were obtained using pagoda flower extracts with various solvents and extraction methods. These samples included nine different extract variations and compounds (1-3) derived from the MMP extract. The variations considered in these samples involved different solvents (methanol, 96% ethanol, and hexane) and extraction methods (maceration, reflux, and microwave), all of which were applied to the flower part of the plant. To analyze these samples ¹H-NMR spectroscopy in combination with chemometric analysis using multivariate techniques such as PCA and CA, played a crucial role. This analysis was essential for studying the grouping and quantitative similarity among these extract variations and for authenticating the target compounds based on the proton resonances present in the samples [23]. Based on the data (Figure 1) obtained from ¹H-NMR at 400 MHz, it was observed that the proton resonances in the RMP, MiMP, MMP, REP, MiEP, and MEP extracts primarily occurred in specific chemical shift regions. These regions included resonances in the range of: δ_H 0.9-1.2 ppm (R-CH₃), δ_H 1.2-1.5 ppm (R₂CH₂), δ_H 1.4-1.9 ppm (R-R₂CH), δ_H 1.5-2.5 ppm (R₂C=CRCHR₂), δ_H 2.0-2.6 ppm (R-CCH₃=O), δ_H 2.2-2.5 ppm (Ar-CH₃), δ_H 2.5-3.0 ppm (R-C=CH), δ_H 3.3-4.0 ppm ((H)R-O-CH₃), δ_H 3.1-3.8 ppm (X-CH₂R; X: Cl, Br, I), δ_H 1-5 ppm (R-OH; R-NH₂), δ_H 4.5-6.0 ppm (R₂C=CRH), δ_H 9.5-10.0 ppm (R-C=O-H). Meanwhile, the RHP, MiHP, and MHP extracts exhibited proton resonances in the same chemical shift regions as mentioned earlier.

Compound (1) stigmasta-5,22,25-trien-3 β -ol displays proton signals at specific chemical shift values based on 1D ¹H NMR and 1D DEPT 135 C-NMR data: δ_H 3.51 ppm (*s*, 1H), δ_H 5.33 ppm (*br d*, 1H), δ_H 5.22 ppm (*dd*, 1H), δ_H 5.16 ppm (*dd*, 1H), δ_H 2.42 ppm (*br q*, 1H), δ_H 4.68 ppm (*br s*, 2H), δ_H 0.69 ppm (*s*, 3H), δ_H 1.02 ppm (*s*, 3H), δ_H 0.99 ppm (*d*, 3H), δ_H 1.63 ppm (*t*, 3H), and δ_H 0.81 ppm (*t*, 3H). Compound (2), 6-Nonadecenoic acid, exhibits proton signals at δ_H 5.33 ppm (*m*, 1H), δ_H 5.24 ppm (*m*, 1H), δ_H 2.21 ppm (*t*, 2H), δ_H 2.0 ppm (*d*, 2H), δ_H 1.62 ppm (*t*, 2H), δ_H 0.87 ppm (*t*, 3H), and a broad singlet at δ_H 1.28 ppm representing 25H. Compound (3), 6,9-Nonadecadienoic acid, methyl ester, features proton signals at δ_H 5.33 ppm (*m*, 2H), δ_H 5.24 ppm (*m*, 2H), δ_H 3.66 ppm (*s*, 3H), δ_H 2.75 ppm (*m*, 2H), δ_H 2.27 ppm (*t*, 2H), δ_H 2.03 ppm (*m*, 1H), δ_H 1.60 ppm (*m*, 2H), δ_H 0.87 ppm (*t*, 3H), δ_H 0.97 ppm (*t*, 1H), and a broad singlet at 1.25 ppm representing 18H. The proton groups that consistently appear in all extract variations, serving as a fingerprint for these variations and compounds, are located at δ_H 5.33 ppm (*m*, 1H) and δ_H 5.24 ppm (*m*, 1H). In the case of compounds (2) and (3), the markers for fatty acids are present at δ_H 1.28 ppm (*br s*, 25H) and δ_H 1.25 ppm (*br s*, 18H) [20, 21], respectively. Additionally, positions at δ_H 0.69 ppm (*s*, 3H) and δ_H 1.02 ppm (*s*, 3H) serve as markers for cholesterol at positions C-18 and C-19 [22].

2.2. Chemometrics

2.2.1. Principal component analysis

PCA is the most widely used multivariate data analysis method [23]. This method is used for sample classification and reduction of samples with similar properties and characteristics based on the measured parameters [24]. Multivariate analysis with a PCA design for sample classification generates statistical data in the form of a scree plot, which aids in understanding the data model, a score plot to visualize data distribution and inter-variable relationships, and a loading plot to reveal the correlation between extract variables. These results were combined with linear regression to identify positive correlations between extracts and linear equations according to grouping [25]. The scree plot analysis should have eigen values that exceed one and be able to explain more than 80% of the data for the data model to be considered excellent and optimal. In this analysis, one eigenvalue exceeds 1, which is PC1 with a value of 10.92, explaining 91% of the data. The scree plot demonstrates that the data follows a normal distribution, as the graph conforms to normality, and each variable is randomly distributed around zero [26].

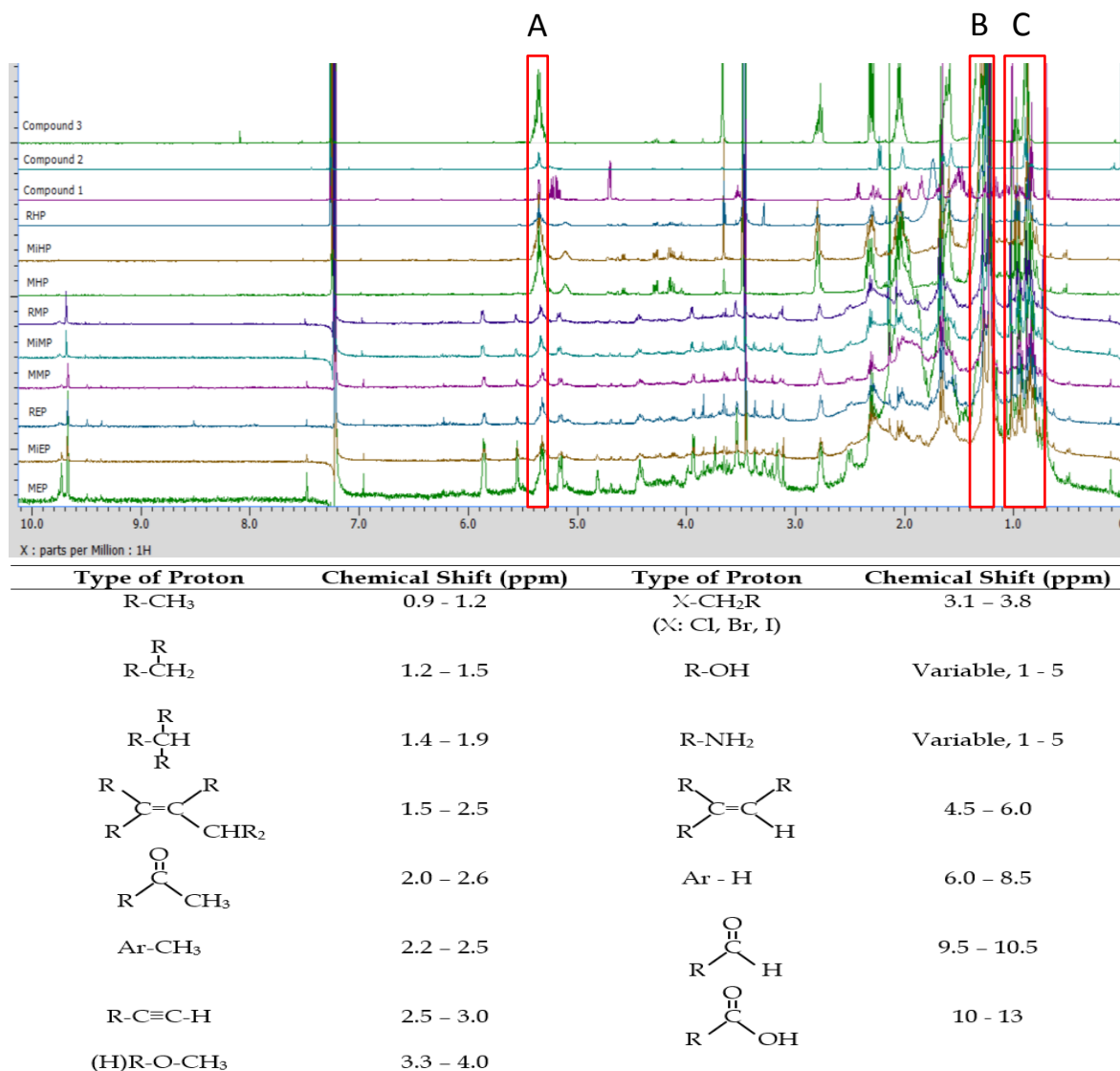


Figure 1. The ¹H NMR spectra of *Clerodendrum paniculatum* extracts are provided for the conditions and identification of compounds (1-3), RHP, MiHP, MHP, RMP, MiMP, MMP, REP, MiEP, and MEP. See refer to the Experimental Procedure section for details. Additionally, (A) serves as a marker for all samples, (B) as a fatty acid marker, and (C) as a cholesterol marker.

The data loading plot (Figure 2) shows that sample variations are divided into two major groups, indicating a positive correlation. Group 1 (represented by the green line) includes RHP, MHP, MiHP, compound (1), and REP, with an influence on PC1 ranging from 0.256 to 0.300 and on PC2 ranging from 0.038 to 0.562. This demonstrates the equation ($y=1.3778x - 1.762$; $R^2 = 0.9338$). Group 2 (represented by the black line) comprises MMP, RMP, MiMP, compound (2), compound (3), MEP, and MiEP, with an influence on PC1 ranging from 0.259 to 0.300, showing the equation ($y=1.139x - 0.8387$; $R^2 = 0.9694$). The data score plot (Figure 3) illustrates the contribution of each variable to PC1 and PC2. The scores indicate the contribution of each variable used for sample classification, with higher variable contributions having a greater impact on the PCA model. The score plot in the results of this study reveals that RHP significantly affects PC1, compound (2) significantly affects PC2, and all variables combined have an 82.2% influence on PC1 and a 10.5% influence on PC2.

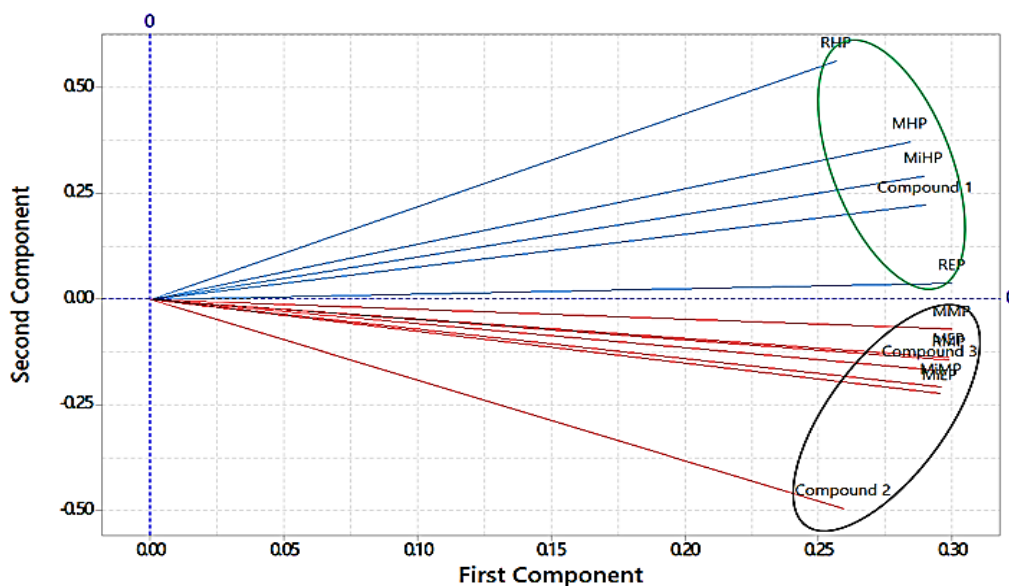


Figure 2. The loading plot illustrates the contribution of variables in the principal component analysis of samples classified under linear correlation. The green line represents group 1, while Group 2 is represented by the black line.

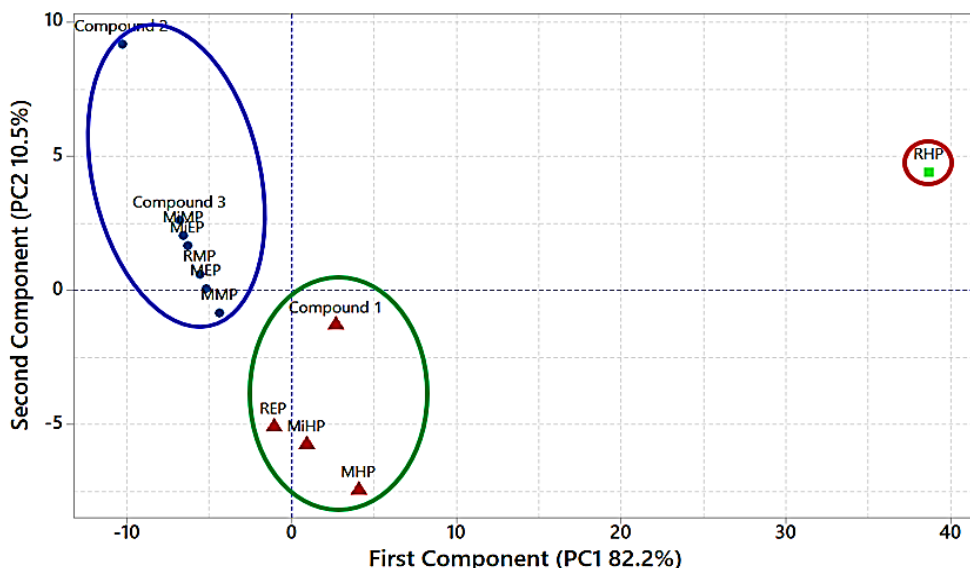


Figure 3. The score plot depicting the classification of samples through principal component analysis shows three groups represented by red, blue, and green lines.

2.2.2. Cluster analysis

CA is a multivariate analysis technique used for clustering based on the Euclidean distance expressed as a percentage of similarities [27, 28]. Similarity data indicate a strong relationship when the percentage of similarity is $\geq 80\%$ [29]. Figure 4 illustrates the dendrogram obtained during variable clustering based on the proton values detected using $^1\text{H-NMR}$ at 400 MHz. The data reveal that it is divided into two clusters: Cluster 1 (92.81%), comprising MMP, RMP, MiMP, compound (2), compound (3), MEP, and MiEP, and Cluster 2 (92.08%), which includes RHP, MHP, MiHP, compound (1), and REP. Based on the data linearity for quantifying extract variations compared to the reference compounds, namely compound (1), compound (2), and compound (3), quantification linearity was found (Table 1). The calibration curve for compound (1) with the highest similarity was observed in the MEP extract ($y = 0.7009x + 1.1428$; $R^2 = 0.9204$; % similarity = 98.26%). For compound (2), the highest similarity was found in the REP extract ($y = 1.1161x - 3.8084$; $R^2 = 0.9189$; % similarity = 94.19%), and for compound (3), the highest similarity was found in the RMP extract ($y = 0.8879x - 0.0971$; $R^2 = 0.9179$; % similarity = 98.13%). However, when compared with all samples (Figure 5), a positive correlation was observed between the variations in the extract and the successfully obtained compounds ($y = 0.9616x - 0.0291$; $R^2 = 0.9734$).

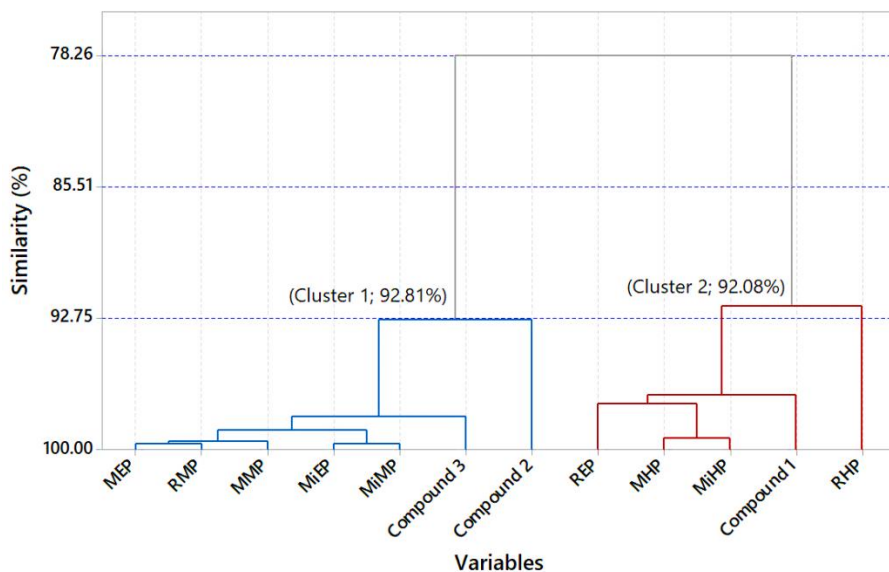


Figure 4. The dendrogram illustrates the classification of samples through cluster analysis, with members of Cluster 1 and Cluster 2 assigned the same colored line for each respective cluster.

Table 1. The linearity for quantitation and the similarity of (1) Stigmasta-5,22,25-trien-3 β -ol, (2) 6-Nonadecenoic acid, and (3) 6,9-Nonadecadienoic acid, methyl ester in the variation of PCP extract.

No	Sample	Isolated Compound	Calibration Curve	R ²	% Similarity
1	MEP	Compound 1	$y = 0.7009x + 1.1428$	0.9204	98.26
2	MiEP	Compound 1	$y = 0.6462x + 1.4723$	0.8902	97.74
3	REP	Compound 1	$y = 0.6292x + 0.8331$	0.9119	98.08
4	MMP	Compound 1	$y = 0.7308x + 0.9808$	0.9198	98.22
5	MiMP	Compound 1	$y = 0.7003x + 1.4124$	0.8942	97.82
6	RMP	Compound 1	$y = 0.7225x + 1.1812$	0.9277	98.36
7	MHP	Compound 1	$y = 0.7465x + 0.2261$	0.8392	95.84
8	MiHP	Compound 1	$y = 0.7863x + 0.3574$	0.8644	96.58
9	RHP	Compound 1	$y = 0.9863x - 2.1226$	0.8525	96.34
10	MEP	Compound 2	$y = 0.998x - 2.1089$	0.8789	96.77
11	MiEP	Compound 2	$y = 0.9437x - 1.715$	0.9078	97.29
12	REP	Compound 2	$y = 1.1161x - 3.8084$	0.9189	94.19
13	MMP	Compound 2	$y = 1.1382x - 2.8658$	0.8701	95.79
14	MiMP	Compound 2	$y = 1.0486x - 1.9764$	0.8639	96.42
15	RMP	Compound 2	$y = 1.0535x - 2.233$	0.8330	95.95
16	MHP	Compound 2	$y = 2.2059x - 9.1776$	0.7700	85.77
17	MiHP	Compound 2	$y = 2.1555x - 8.3511$	0.7703	87.66
18	RHP	Compound 2	$y = 2.5039x - 13.225$	0.8297	78.26
19	MEP	Compound 3	$y = 0.8342x - 0.0541$	0.8576	96.98
20	MiEP	Compound 3	$y = 0.7665x + 0.3471$	0.8313	96.18
21	REP	Compound 3	$y = 0.8253x - 0.8147$	0.8496	97.58
22	MMP	Compound 3	$y = 0.9122x - 0.4126$	0.8933	98.98
23	MiMP	Compound 3	$y = 0.8538x + 0.2039$	0.8760	97.19
24	RMP	Compound 3	$y = 0.8879x - 0.0971$	0.9179	98.13
25	MHP	Compound 3	$y = 1.3131x - 3.1403$	0.7550	94.79
26	MiHP	Compound 3	$y = 1.247x - 2.3584$	0.8139	96.12
27	RHP	Compound 3	$y = 1.9551x - 8.3529$	0.9288	86.92

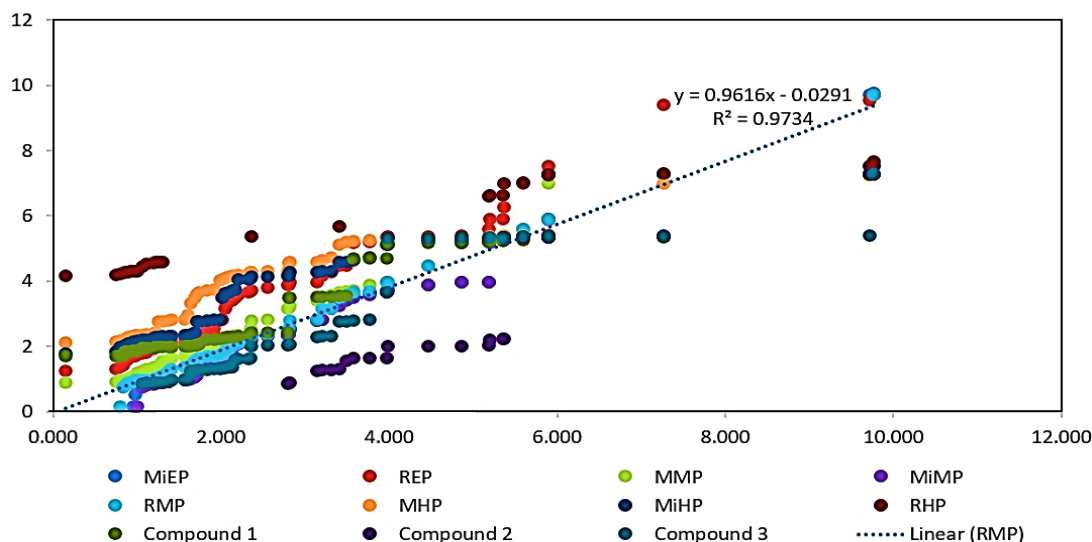


Figure 5. The variations in the extract and the obtained compounds indicate a positive correlation relationship.

2.3. Isolation of compounds

The MMP extract with a total quantity of 95.16 g was chosen for the subsequent isolation of compounds. The procedure involved three rounds of partitioning using a mixture of hexane and methanol-water (1:1), each time employing 250 ml solvent. The obtained MeOH and hexane extracts weighed 68.76 grams and 17.4 grams, respectively. To separate the compounds in the hexane layer, a combination of various chromatography techniques was applied, leading to the isolation of the following compounds: (1) stigmasta-5,22,25-trien-3 β -ol, (2) 6-nonadecenoic acid, and (3) 6,9-nonadecadienoic acid, methyl ester. Detailed 1D spectroscopic, 2D NMR, and mass spectrometry data were also reported for these compounds.

Compound (1) is a white, non-crystalline powder belonging to the steroid group. Its molecular formula is $C_{29}H_{46}O$, as indicated by the mass spectrometry data (m/z 410 [M^+]) in Figure 6. The 1H NMR spectroscopy data, presented in Table 2 show various signals. Notably, there are five methyl group signals at specific chemical shift positions: δ_H 0.69 ppm (3H, s), δ_H 1.02 ppm (3H, s), δ_H 0.99 ppm (3H, d), δ_H 1.63 ppm (3H, t), and δ_H 0.81 ppm (3H, t). Additionally, there are proton methine signals at δ_H 5.33 ppm (1H, *br d*, $J=5.50$ Hz), δ_H 5.22 ppm (1H, *dd*, $J=8.24$ Hz), δ_H 5.16 ppm (1H, *dd*, $J=8.24$ Hz), δ_H 2.42 ppm (1H, *br q*), and δ_H 3.51 ppm (1H, s). These proton signals are attributed to hydroxyl groups or methylene protons, as confirmed by the DEPT 135 data, providing insight into carbon positions. Furthermore, the ^{13}C NMR spectrum indicates the presence of 29 carbon atoms within the compound. DEPT 135 data helps determine the carbon functionalities. Specific carbon signals are observed at δ_C 71.88 ppm carbon with a hydroxyl group, δ_C 121.77 ppm, δ_C 137.28 ppm, δ_C 130.10 ppm, and δ_C 109.59 ppm carbons involved in double bonds, and δ_C 140.8 ppm, δ_C 36.58 ppm, δ_C 42.33 ppm, and δ_C 148.78 ppm carbons without associated protons.

The two-dimensional NMR data, including the HMQC and HMBC spectra in Figure 6, revealed significant correlations between hydrogen and carbon atoms, as indicated by the blue lines: methyl protons with a chemical shift at δ_H 1.02 ppm (3H, s) were correlated with carbon atoms at δ_C 36.58 ppm (C-10), δ_C 37.32 ppm (C-1), δ_C 50.21 ppm (C-9), and δ_C 140.8 ppm (C-5). Methyl protons with a chemical shift at δ_H 0.99 ppm (3H, d) were correlated with carbon atoms at δ_C 40.28 ppm (C-20), δ_C 55.94 ppm (C-17), and δ_C 137.28 ppm (C-22). Methyl protons with a chemical shift at δ_H 0.69 ppm (3H, s) were correlated with carbon atoms at δ_C 55.94 ppm (C-17), δ_C 42.33 ppm (C-13), and δ_C 39.74 ppm (C-12). Additionally, protons with a chemical shift at δ_H 0.81 ppm (3H, t) and carbon at δ_C 12.13 ppm were correlated with carbon atoms at δ_C 25.78 ppm (C-28) and δ_C 52.06 ppm (C-24). Furthermore, protons with a chemical shift at δ_H 1.63 ppm (3H, t) and carbon at δ_C 20.30 ppm were correlated with carbon atoms at δ_C 52.06 ppm (C-24), δ_C 148.78 ppm (C-25), and δ_C 109.59 ppm (C-26). The methylene protons with a broad singlet at δ_H 4.68 ppm (2H) were correlated with carbon atoms at δ_C 52.06 ppm (C-24) and δ_C 20.30 ppm (C-27). These correlations provide essential insights into the chemical structure of the compound and the connections between different functional groups.

The 1H - 1H Cosy correlation data shown in Figure 6, indicated by the black lines, revealed the following proton correlations: Proton H3 with a chemical shift of δ_H 3.51 ppm (1H, s) was correlated with protons H2 and H4. Proton H6 with a chemical shift of δ_H 5.33 ppm (1H, *br d*) was correlated with proton H7. Proton H22 with a chemical shift of δ_H 5.16 ppm (1H, *dd*) was correlated with proton H20. Proton H20 with a chemical shift of δ_H 4.99 ppm (1H, *dd*) was correlated with proton H17 and H21. In addition, the combined

data from 1D and 2D NMR, as well as ESI⁺ MS analysis, confirmed that this previously unreported compound in this plant species is a steroid known as (1) stigmasta-5,22,25-trien-3 β -ol with the steroid framework positioned at carbons C1 - C19, which has been previously characterized. It is noteworthy that this compound has been documented in the same genus but in different species, including *Clerodendrum viscosum* [30], *Clerodendrum scandens* [31], *Clerodendrum splendens* [32], *Clerodendron brachyanthum* [33], *Clerodendrum inerme* [34], and *Clerodendrum serratum* [35]. It was first isolated from the leaf parts of *Alangium lamarckii* [45] and *Albizia ferruginea* [46]. However, this is the first reported occurrence of this compound in this plant species.

Compound (2), 6-nonadecenoic acid, is a yellowish oil. Mass spectrometry data (DART⁺ MS) confirmed a molecular weight of m/z 296 [M⁺], which corresponds to the chemical formula C₁₉H₃₆O₂, as depicted in Figure 6. The spectroscopic data from ¹H NMR, ¹³C NMR, DEPT 135, and 2D NMR, as outlined in Table 2, provide the following insights: One group of methyl protons at δ_H 0.87 ppm (3H, *t*) with a corresponding carbon at δ_C 14.13 ppm. A set of fifteen methylene protons at δ_H 1.28 ppm (25H, *br s*), δ_H 2.21 ppm (2H, *t*), δ_H 2.0 ppm (2H, *d*), and δ_H 1.62 ppm (2H, *t*), with their respective carbon resonances at δ_C 22.69 ppm, δ_C 25.51 ppm, δ_C 27.16 ppm, δ_C 27.22 ppm, δ_C 29.11 ppm, δ_C 29.24 ppm, δ_C 29.32 ppm, δ_C 29.20 ppm, δ_C 29.49 ppm, δ_C 29.32 ppm, δ_C 29.52 ppm, δ_C 29.70 ppm, δ_C 29.76 ppm, δ_C 31.91 ppm, and δ_C 35.89 ppm. Furthermore, there are two methine protons at δ_H 5.33 ppm (1H, *m*) with a corresponding carbon at δ_C 130.01 ppm and δ_H 5.24 ppm (1H, *m*) with a corresponding carbon at δ_C 129.73 ppm. In addition, there is a carbon lacking a proton at δ_C 175.43 ppm, which indicates its association with a hydroxyl group, as confirmed by 2D NMR data. This information collectively provides a comprehensive understanding of the compound structure and is consistent with data obtained from ¹³C NMR, DEPT 135, DART⁺ MS, and 2D NMR analyses.

The two-dimensional NMR data, including the HMQC and HMBC spectra in Figure 6, reveal correlations between hydrogen and carbon atoms, indicated by the blue lines: methyl protons with a chemical shift at δ_H 0.87 ppm (3H, *t*) correlate with carbon atoms at δ_C 22.69 ppm (C-18) and δ_C 31.91 ppm (C-17). Protons with a chemical shift at δ_H 2.21 ppm (2H, *t*) correlate with carbon atoms at δ_C 175.43 ppm (C-1), δ_C 25.51 ppm (C-3), and δ_C 29.52 ppm (C-4). Protons with a chemical shift at δ_H 2.0 ppm (2H, *d*) correlate with carbon atoms at δ_C 130.01 ppm (C-6) and δ_C 129.73 ppm (C-7). Protons with a chemical shift at δ_H 1.62 ppm (2H, *t*) correlate with carbon at δ_C 29.52 ppm (C-4). Protons with a chemical shift at δ_H 1.28 ppm (2H, *br s*) correlate with carbon at δ_C 31.91 ppm (C-17). Additionally, the ¹H-¹H Cosy correlation data in Figure 6, indicated by the black lines, show correlations between protons: Proton H2 (δ_H 2.21 ppm, 2H, *t*) correlates with H3 (δ_H 1.62 ppm, 2H, *t*), H4 (δ_H 1.28 ppm, 2H, *br s*), H5, and H6 (δ_H 5.33 ppm, 1H, *m*). On the basis of data from 1D and 2D NMR, DEPT 135, and DART⁺ MS, it is confirmed that this compound, previously unreported in the *Clerodendrum* genus, is a phospholipid fatty acid known as (2) 6-nonadecenoic acid. Notably, although this compound has been found in other plant species, it had not been previously reported within the *Clerodendrum* genus before this publication. It was first documented in *Caribbean sponge* species, including *Geodia gibberosa* [36], *Cinachyrella* aff. *schulzei* keller [37], *Polygonatum odoratum* [38], and *Calyx odatypa* [39].

Compound (3) 6,9-nonadecadienoic acid methyl ester is a yellow oil. Mass spectrometry data (DART⁺ MS) revealed a molecular weight of m/z 308 [M⁺], which corresponds to the chemical formula C₂₀H₃₆O₂, as depicted in Figure 6. The ¹H NMR, ¹³C NMR, and DEPT 135 spectroscopy data presented in Table 2 provide the following information: There are two sets of methyl protons at δ_H 0.87 ppm (3H, *t*) with corresponding carbons at δ_C 14.08 ppm, and δ_H 3.66 ppm (3H, *s*) as a methoxy group with a carbon at δ_C 174.34 ppm. Thirteen methylene protons at δ_H 1.25 ppm (18H, *br s*), δ_H 2.75 ppm (2H, *m*), δ_H 2.27 ppm (2H, *t*), δ_H 1.60 ppm (2H, *m*), and δ_H 2.03 ppm (2H, *m*), with their respective carbon shifts at δ_C 22.58 ppm, δ_C 22.70 ppm, δ_C 24.95 ppm, δ_C 25.63 ppm, δ_C 27.21 ppm, δ_C 29.12 ppm, δ_C 29.16 ppm, δ_C 29.35 ppm, δ_C 29.59 ppm, δ_C 29.69 ppm, δ_C 31.54 ppm, δ_C 34.11 ppm, and δ_C 51.45 ppm. There are four methine protons at δ_H 5.33 ppm (2H, *m*) with corresponding carbons at δ_C 130.06 ppm and δ_C 130.23 ppm, and δ_H 5.24 ppm (2H, *m*) with corresponding carbons at δ_C 127.91 ppm and δ_C 128.04 ppm. Furthermore, a carbon without a proton at δ_C 174.34 ppm was associated with a methoxy group, as confirmed by 2D NMR data.

The two-dimensional NMR data, including the HMQC and HMBC spectra in Figure 6, reveal correlations between hydrogen and carbon atoms, represented by blue lines. Methyl protons at δ_H 3.66 ppm (3H, *s*) correlate with carbon at δ_C 174.34 ppm (C-1). Protons at δ_H 2.27 ppm (2H, *t*) correlate with carbon at δ_C 174.34 ppm (C-1), δ_C 24.95 ppm (C-3), and δ_C 29.35 ppm (C-4). Methyl protons at δ_H 0.87 ppm (3H, *t*) correlate with carbon at δ_C 31.54 ppm (C-17) and δ_C 22.70 ppm (C-18). Methine protons at δ_H 5.33 ppm (2H, *m*) correlate with carbon at δ_C 27.21 ppm (C-5). Methine protons at δ_H 5.24 ppm (2H, *m*) correlate with carbon at δ_C 25.69 ppm (C-8). Protons at δ_H 2.75 ppm (2H, *m*) correlate with carbon at δ_C 127.91 ppm (C-9). Protons at δ_H 2.03 ppm (2H, *m*) correlate with carbon at δ_C 29.35 ppm (C-4), δ_C 130.23 ppm (C-6), and δ_C 130.23 ppm (C-7).

Protons at δ_H 1.60 (2H, *m*) correlate with carbon at δ_C 174.34 ppm (C-1), δ_C 34.11 ppm (C-2), and δ_C 29.35 ppm (C-4). Protons at δ_H 1.25 ppm (2H, *br s*) correlate with carbon at δ_C 31.54 ppm (C-17).

The correlation data between protons using 1H - 1H Cosy in Figure 6, indicated by the black lines, reveals the following correlations: Proton H2 (δ_H 2.27 ppm, 2H, *t*) correlates with H3 (δ_H 1.60 ppm, 2H, *m*). H3 correlates with H4 (δ_H 1.25 ppm, 2H, *br s*). H4 correlates with H5 (δ_H 2.03 ppm, 2H, *m*). H5 correlates with H6 (δ_H 5.33 ppm, 2H, *m*). H9 (δ_H 5.24 ppm, 2H, *m*) correlates with H8 (δ_H 2.75 ppm, 2H, *m*). H19 (δ_H 0.87 ppm, 3H, *t*) correlates with H18 (δ_H 2.03 ppm, 2H, *m*). Based on these data, it is confirmed that this compound, previously unreported in the *Clerodendrum* genus, is a phospholipid fatty acid known as (3) 6,9-Nonadecadienoic acid, methyl ester. This compound had not been reported within the *Clerodendrum* genus before this publication.

Table 2. The data includes 1H NMR, ^{13}C NMR, and DEPT 135 spectra of (1) Stigmasta-5,22,25-trien-3 β -ol, (2) 6-Nonadecenoic acid, and (3) 6,9-Nonadecadienoic acid, methyl ester recorded at 400 MHz in $CDCl_3$.

Compound (1)		Compound (2)		Compound (3)	
Observed ^{13}C (ppm)	Observed 1H and DEPT (ppm)	Observed ^{13}C (ppm)	Observed 1H and DEPT (ppm)	Observed ^{13}C (ppm)	Observed 1H and DEPT (ppm)
37.33, CH ₂	<i>septet</i> , 3.51 (1H)	14.13	<i>m</i> , 5.33 (1H)	14.08	<i>m</i> , 5.33 (2H)
31.97, CH	<i>br d</i> , 5.33 (1H)	22.69	<i>m</i> , 5.24 (1H)	14.13	<i>m</i> , 5.24 (2H)
71.88, CH	<i>dd</i> , 5.22 (1H)	25.51	<i>t</i> , 2.21 (2H)	22.58	<i>s</i> , 3.66 (3H)
42.37, CH ₂	<i>dd</i> , 5.16 (1H)	27.16	<i>d</i> , 2.0 (2H)	22.70	<i>m</i> , 2.75 (2H)
140.8, C	<i>br q</i> , 2.42 (1H)	27.22	<i>t</i> , 1.62 (2H)	24.95	<i>t</i> , 2.27 (2H)
121.77, CH	<i>br s</i> , 4.68 (2H)	29.11	<i>t</i> , 0.87 (3H)	25.63	<i>m</i> , 2.03 (1H)
31.74, CH ₂	<i>s</i> , 0.69 (3H)	29.24	<i>br s</i> , 1.28 (25H)	27.21	<i>m</i> , 1.60 (2H)
31.97, CH ₂	<i>s</i> , 1.02 (3H)	29.32		29.12	<i>t</i> , 0.87 (3H)
50.22, CH	<i>d</i> , 0.99 (3H)	29.20		29.16	<i>t</i> , 0.97 (1H)
36.59, C	<i>t</i> , 1.63 (3H)	29.49		29.35	<i>br s</i> , 1.25 (18H)
21.14, CH ₂	<i>t</i> , 0.81(3H)	29.32		29.59	
40.27, CH		29.52		29.69	
42.33, C		29.70		31.54	
56.92, CH		29.76		34.11	
24.39, CH ₂		31.91		51.45	
28.79, CH ₂		35.89		127.91	
55.94, CH		130.01		128.04	
12.13, CH ₃		129.73		130.06	
19.47, CH ₃		175.45		130.23	
39.74, CH ₂				174.34	
109.59, CH ₂					
137.28, CH					
130.1, CH					
52.07, CH					
148.70, C					
20.87, CH ₃					
20.30, CH ₃					
25.78, CH ₂					
12.22, CH ₃					

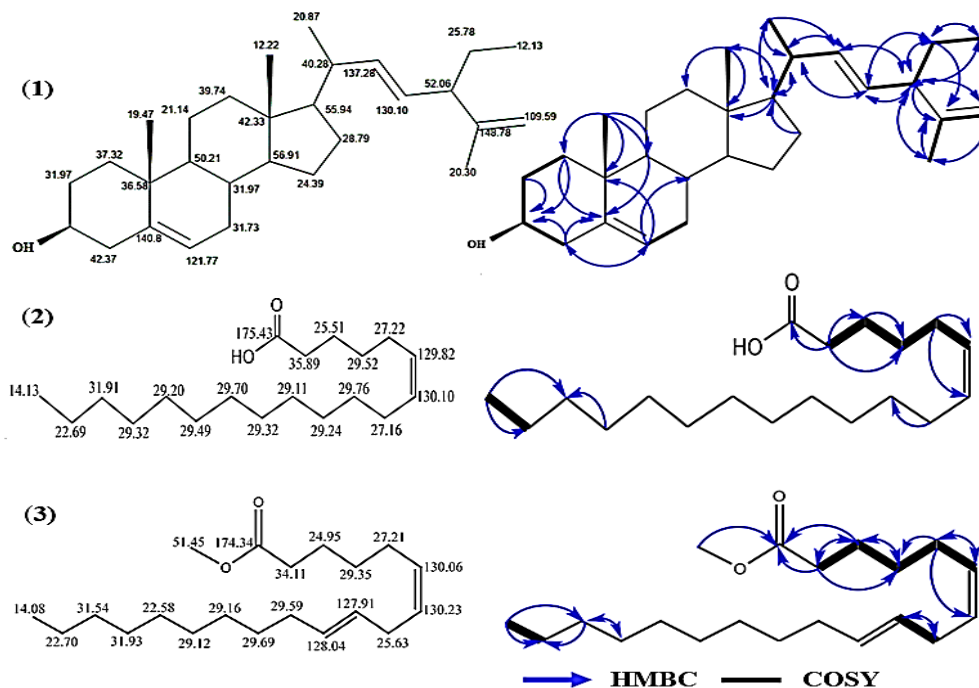


Figure 6. The structure of compounds (1) Stigmasta-5,22,25-trien-3 β -ol, (2) 6-Nonadecenoic acid, and (3) 6,9-Nonadecadienoic acid, methyl ester, along with their two-dimensional proton correlations

2.4. Cytotoxicity Activity

The preliminary test results of the (MHP) maceration hexane flower extract, (MMP) maceration methanol flower extract, (MHL) maceration hexane leaf extract, and (MML) maceration methanol leaf extract against cytotoxic cancer cells with 20 $\mu\text{g}/\text{mL}$ showed that the percentage growth of all cancer cells was > 89.6 %. These results indicate that the initial extracts from the flower and leaf parts of this plant, extracted using methanol and hexane solvents with maceration as the extraction method, exhibit low inhibitory effects on various tested cancer cell types, including KB, KB-VIN, A549, MDA-MB-231, and MCF-7, compared with the negative control DMSO at 0.20%, which fully inhibits the growth of cancer cells (100%).

Based on the existing literature, MML has IC_{50} values of 196.55 $\mu\text{g}/\text{ml}$ for inhibiting MCF-7 breast cancer cells, 190.21 $\mu\text{g}/\text{ml}$ for inhibiting KB cancer cells, and 118.77 $\mu\text{g}/\text{ml}$ for inhibiting A549 cancer cells. In contrast, the positive control paclitaxel had respective values of 298.86 $\mu\text{g}/\text{ml}$, 264.71 $\mu\text{g}/\text{ml}$, and 273.25 $\mu\text{g}/\text{ml}$ [40]. In cytotoxicity testing using the Brine Shrimp Test (BST), the MHP extract had an LC_{50} of 0.02 $\mu\text{g}/\text{ml}$, MMP had an LC_{50} of 1.94 $\mu\text{g}/\text{ml}$, MHL had an LC_{50} of 1.48 $\mu\text{g}/\text{ml}$, and MML had an LC_{50} of 3.09 $\mu\text{g}/\text{ml}$. These results indicate toxic effects on *Artemia salina* when incubated for 24 h [1].

Compounds isolated from this plant include compound (1), with the synonym 22-dehydroclerosterol (25 $\mu\text{mol}/\text{L}$), which demonstrates 56.10% inhibition of proliferation in ER⁺ breast cancer (MCF-7) cells [41]. However, it does not exhibit activity against human colon adenocarcinoma (SW620), lung bronchus carcinoma (ChaG0-K-1), hepatocellular carcinoma (HepG2), gastric carcinoma (KATO-III), or human breast cancer cell line (BT-474) [42]. On the other hand, compound (2) with the synonym 6Z-nonadecenoic acid or (Z)-6-Nonadecenoic acid does not show anticancer activity but possesses other properties, such as antifungal effects. Its derivative, 4R-hydroxy-5S-cysteinylglycyl-6Z-nonadecenoic acid, acts as an antagonist to the mediators LTD₄, LTC₄, and LTE₄ in the respiratory system [43]. Compound (3) also lacks anticancer activity, but its derivative, nonadecenoic acid methyl ester, exhibits anti-inflammatory, anti-acne, and insecticidal effects [44].

3. CONCLUSION

Fingerprint profiling markers in various *Clerodendrum paniculatum* flower extracts using different solvents (hexane, methanol, and 96% ethanol) and extraction methods (reflux, microwave-assisted extraction, and maceration), as well as the isolated compounds (1), (2), and (3), are located at δ_{H} 5.33 ppm (*m*, 1H) and δ_{H} 5.24 ppm (*m*, 1H). The study identified specific markers for compounds and various extracts were fatty acids, and cholesterol. Principal component analysis revealed distinct groupings among the extracts, while cluster analysis further confirmed these groupings. Calibration curves demonstrated

<https://doi.org/10.12991/jrespharm.1693824>

J Res Pharm 2025; 29(3): 971-984

quantification linearity for isolated compounds in specific extracts. Furthermore, preliminary testing suggested weak inhibitory effects on various cancer cell lines. This comprehensive analysis provides valuable insights into the chemical composition and potential bioactivity of *Clerodendrum paniculatum* flower extracts, laying a foundation for further exploration in pharmaceutical and medicinal applications.

4. MATERIALS AND METHODS

4.1 Materials

A sample of PCP (*Clerodendrum paniculatum*) flower approximately 10 kg was collected in the city of Masamba, North Luwu District, South Sulawesi Province, Indonesia. Plant identification was conducted at the Botanical Laboratory, Department of Biology, Faculty of Mathematics and Natural Sciences, Universitas Negeri Makassar, Indonesia, with reference number No: 046/SKAP/LAB.BIOLOGI/IV/2018. The preparation process involved sorting to remove any moldy or damaged flower parts. The flower parts were then cut into small pieces and subjected to a drying process using an oven with a temperature range of 40-50 °C for 3 days. The dried material was packed, supplemented with desiccant (silica beads), coarsely shredded, and prepared for the extraction process [1, 19].

4.2 Extraction and isolation

As many as 25 g of PCP dried flower were extracted using different solvents (hexane, methanol, and 96% ethanol) and subjected to extraction methods (reflux, microwave-assisted extraction, and maceration). The solid-to-solvent ratio was maintained at 1:10 (w/v). The resulting liquid extracts were passed through filter paper in combination with a vacuum pump. Then, all of the extracts were concentrated using a rotary evaporator IKA RV 3 V with a speed range specification of 60 – 80 rpm, permissible ambient temperature of 40 – 60 °C for 2-3 h, and under vacuum conditions. The pagoda flower extracts obtained from this process were categorized as follows: reflux hexane flower (RHP) extract, microwave-assisted hexane flower (MiHP) extract, maceration hexane flower (MHP) extract, reflux methanol flower (RMP) extract, microwave-assisted methanol flower (MiMP) extract, maceration methanol flower (MMP) extract, reflux 96% ethanol flower (REP) extract, microwave-assisted 96% ethanol flower (MiEP) extract, and maceration 96% ethanol flower (MEP) extract. This process outlines the extraction and categorization of pagoda flower extracts based on variations in solvents and extraction methods.

A total of 95.16 g extract from the MMP was partitioned using hexane and a methanol-water mixture (1:1) in three separate 250 ml portions. The resulting MeOH and hexane extracts yielded 68.76 grams and 17.4 grams, respectively. The hexane-partitioned extract was separated using a normal phase (NP) silica chromatography column. This separation involved a mobile phase consisting of hexane and ethyl acetate with the following ratios: (8:1) 5 times, (6:1) 9 times, (4:1) 10 times, (1:1) 2 times, and (1:5) 2 times. In addition, 650 ml ethyl acetate and 1050 ml methanol were used once in the process. From this fractions were obtained: the A - P fraction and fraction (P), weighing 0.2521 grams, which was washed with hexane. During this process, a portion soluble in hexane (A) was isolated and weighed 0.0089 g. Furthermore, the insoluble part in hexane (B) was 0.0153 g identified as compound (1).

Fraction (C), weighing 1.2992 g, was subjected to normal phase (NP) silica chromatography. The mobile phase consisted of hexane and ethyl acetate with the following ratios: (20:1) twice, (15:1) 3 times, (10:1) 2 times, (5:1) 3 times, and (1:1) 3 times. In addition, a one-time use of 300 ml of ethyl acetate and 300 ml methanol was used in the process. From this, an A - G subfraction was obtained, with subfraction (E) weighing 0.0134 g. To isolate compound (2), further purification was performed using Preparative Thin-Layer Chromatography (PTLC) on NP silica with a mobile phase of hexane and ethyl acetate (5:1), resulting in a yellowish oil compound weighing 0.0010 g.

Fraction (B), consisting of 0.1542 g, was processed using a normal phase (NP) silica chromatography column. The mobile phase used was a combination of hexane and ethyl acetate with a ratio of (20:1) 2 times. In addition, 200 mL of ethyl acetate and 300 mL of methanol were used once in the process. From this, an A - F subfraction was obtained, with subfraction (B) resulted in 0.0207 g. Subsequently, normal phase preparative TLC was employed by using a mobile phase of hexane and ethyl acetate (8:1) to isolate compound (3), resulting in a yellowish oil compound (0.0023 g).

4.3 Cytotoxicity activity

In the initial cytotoxicity tests, various extracts from the Pagoda plant were used. These extracts included maceration methanol and hexane extracts from both leaves and flowers. Each of these extracts was weighed at 1 mg and prepared at a concentration of 20 µg/ml. Dimethyl sulfoxide (DMSO) was used as the

negative control at a concentration of 0.1 % v/v. DMSO at this concentration did not show any inhibitory effect on cancer cells, as previously reported [47, 48]

The tests involved five different lines of human tumor cells: KB (originally isolated from epidermoid carcinoma of the nasopharynx), KB-VIN (a vincristine-resistant subline of KB displaying multidrug resistance due to the overexpression of P-glycoprotein), A549 (lung carcinoma), MDA-MB-231 (characterized by estrogen receptor-negative, progesterone receptor-negative, and HER2-negative breast cancer), and MCF-7 (characterized by estrogen receptor-positive and HER2-negative breast cancer). These cell lines were obtained from the Lineberger Comprehensive Cancer Center (UNC-CH) or ATCC. Following a 72-h incubation period, 10% trichloroacetic acid was added, and the sulforhodamine B assay was performed at a concentration of 0.04%. The cell growth percentage was calculated for each tested well and compared with the control wells. This calculation was performed using the following formula: (Average absorbance of test wells × 100) / Average absorbance of control wells, as previously described [49, 50].

4.4 Analysis of fingerprinting profiling extracts

The analysis of fingerprinting profiles for the extracts involved nine different variations of PCP extracts and three compounds, which were prepared using various solvents and extraction methods. Compounds (1), (2), and (3) were analyzed by ¹H-NMR spectroscopy at 400 MHz using a JEOL Delta® instrument. For this analysis, 5 mg of each sample was mixed with 5 ml of deuterated chloroform (CDCl₃). The NMR system met specific criteria, including a minimum spin rate of 15 Hz and a pressure of 260 MPa. A total of 60 scans were conducted over a 5-min period, and the data were processed using JEOL Delta v5.3.3 software for spectrum analysis of the samples.

4.5 Chemometrics analysis

The chemometric analysis involved determining the chemical shift values of the nine different PCP extract variations and three compounds, considering various solvents and extraction methods. Compounds (1), (2), and (3) were identified on the basis of measurements obtained from ¹H-NMR spectra and were subjected to statistical analysis using chemometric techniques. The software used for this analysis was Minitab® version 18, developed by Minitab Incorporation in the USA. Multivariate analysis methods were employed for data interpretation and pattern recognition, including principal component analysis (PCA) and cluster analysis (CA).

Acknowledgements: The authors would like to thank this research was supported scholarship by Kanazawa University Short-Term Exchange Program for Science and Technology (KUEST) 2019 – 2020 from Japan Student Services Organization (JASSO). We are grateful to Dr. Masuo Goto (The University of North Carolina at Chapel Hill, US) for performing the cytotoxicity assay and for providing the essential laboratory facilities.

Author contributions: Concept – B.Y., M.A.; Design – B.Y., A.P., M.A.S; Supervision – A.R., K.N., Y.S; Resources – B.Y., G.A; Materials – K.N., Y.S; Data Collection and/or Processing – B.Y.; Analysis and/or Interpretation – B.Y., M.R., A.R., G.A.; Literature Search – B.Y., M.R., M.A; Writing – B.Y.; Critical Reviews – B.Y., M.R., K.N., Y.S., A.R., G.A.

Conflict of interest statement: The authors declare no conflict of interest.

REFERENCES

- [1] Yasir B, Astuti AD, Raihan M, Natzir R, Subehan S, Rohman A, Alam G. Optimization of Pagoda (*Clerodendrum paniculatum* L.) extraction based by analytical factorial design approach, its phytochemical compound, and cytotoxicity activity. *Egypt J Chem.* 2022; 65(9): 421-430. <https://doi.org/10.21608/EJCHEM.2022.82407.4060>
- [2] Kuźma Ł, Gomulski J. Biologically active diterpenoids in the *Clerodendrum* Genus – A Review. *Int J Mol Sci.* 2022; 23(19): 11001. <https://doi.org/10.3390/ijms231911001>
- [3] Wang JH, Luan F, He XD, Wang Y, Li MX. Traditional uses and pharmacological properties of *Clerodendrum* phytochemicals. *J Tradit Complement Med.* 2018; 8(1): 24-38. <https://doi.org/10.1016/j.jtcme.2017.04.001>
- [4] Priyanka K, Kuppast IJ, Gururaj SV, Chethan IA. Screening of aerial parts of the plant *Clerodendrum paniculatum* Linn for anti-convulsant activity. *Res J Pahrmacol Pharmacodyn.* 2019; 11(1): 1-4. <https://doi.org/10.5958/2321-5836.2019.00001.6>
- [5] Prathima TS, Ahmad MG, Karuppasamy R, Chanda K, Balamurali MM. Investigation on phyto- active constituent of *Clerodendrum paniculatum* as therapeutic agent against viral diseases. *ChemistrySelect.* 2023; 8(4): ae202203932. <https://doi.org/10.1002/slct.202203932>
- [6] Varghese S, Kannappan P, Kanakasabapathi D, Madathil S, Perumalsamy M. Antidiabetic and antilipidemic effect of *Clerodendrum paniculatum* flower ethanolic extract. An *in vivo* investigation in Albino Wistar rats. *Biocatal Agric Biotechnol.* 2021; 36: 102095. <https://doi.org/10.1016/j.bcab.2021.102095>
- [7] Kopilakkal R, Musuvathi BM. Evaluation of hepatoprotective activity of *Clerodendrum paniculatum* leaf on carbon tetrachloride-induced liver toxicity model in swiss albino rats and its characterization by GC-MS. *Endocr Metab Immune Disord Drug Targets.* 2020; 20(7): 1097-1109. <https://doi.org/10.2174/1871530320666200312152331>

- [8] Kopilakkal R, Chanda K, Balamurali MM. Hepatoprotective and antioxidant capacity of *Clerodendrum paniculatum* flower extracts against carbon tetrachloride-induced hepatotoxicity in rats. *ACS omega*. 2021; 6(40): 26489-26498. <https://doi.org/10.1021/acsomega.1c03722>
- [9] Pertiwi D, Sitorus P, Hafiz I, Satria D. Analysis of component and antibacterial activity of ethanol extract and ethyl acetate fraction of Pagoda (*Clerodendrum paniculatum* L.) leaves against *Pseudomonas aeruginosa* and MRSA. *Res J Pharm Technol*. 2022; 15(7): 3047-3050. <https://doi.org/10.52711/0974-360X.2022.00509>
- [10] Sindhu TJ, Akhilesh KJ, Jose A, Binsiya KP, Thomas B, Wilson E. Antiviral screening of Clerodol derivatives as COV 2 main protease inhibitor in novel corona virus disease: In silico approaches. *Asian J Pharm Technol*. 2020; 10(2): 60-64. <https://doi.org/10.5958/2231-5713.2020.00012.4>
- [11] Hegde NP, Hungund BS. Phytochemical profiling of *Clerodendrum paniculatum* leaf extracts: GC-MS, LC-MS analysis and comparative evaluation of antimicrobial, antioxidant & cytotoxic effects. *Nat Prod Res*. 2023;37(17):2957-2964. <https://doi.org/10.1080/14786419.2022.2140339>
- [12] Arba M, Arfan A, Yamin Y, Zubair MS. The potential of *Clerodendrum paniculatum* leaves fraction as a 3-Chymotrypsin-Like (3CL) protease inhibitor of SARS-CoV-2. *Indones J Chem*. 2023; 23(3): 770-781. <https://doi.org/10.22146/ijc.81447>
- [13] Rinschen MM, Ivanisevic J, Giera M, Siuzdak G. Identification of bioactive metabolites using activity metabolomics. *Nat Rev Mol Cell Biol*. 2019; 20(6): 353-367. <https://doi.org/10.1038/s41580-019-0108-4>
- [14] Kharbach M, Marmouzi I, El Jemli M, Bouklouze A, Heyden YV. Recent advances in untargeted and targeted approaches applied in herbal-extracts and essential-oils fingerprinting-A review. *J Pharm Biomed Anal*. 2020; 177: 112849. <https://doi.org/10.1016/j.jpba.2019.112849>
- [15] Olawode EO, Tandlich R, Cambray G. ¹H-NMR profiling and chemometric analysis of selected honeys from South Africa, Zambia, and Slovakia. *Molecules*. 2018; 23(3): 578. <https://doi.org/10.3390/molecules23030578>
- [16] Villa-Ruano N, Ramírez-Meraz M, Méndez-Aguilar R, Zepeda-Vallejo LG, Álvarez-Bravo A, Pérez-Hernández N, Becerra-Martínez E. ¹H NMR-based metabolomics profiling of ten new races from *Capsicum annuum* cv. serrano produced in Mexico. *Food Res Int*. 2019; 119: 785-792. <https://doi.org/10.3390/molecules23030578>
- [17] Deborde C, Fontaine JX, Jacob D, Botana A, Nicaise V, Richard-Forget F, Lecomte S, Decourtil C, Hamade K, Mesnard F, Moing A, Molinié R. Optimizing 1D ¹H-NMR profiling of plant samples for high throughput analysis: Extract preparation, standardization, automation and spectra processing. *Metabolomics*. 2019 ;15(3):28. <https://doi.org/10.1007/s11306-019-1488-3>
- [18] Riswanto FDO, Windarsih A, Lukitaningsih E, Rafi M, Fadzilah NA, Rohman A. Metabolite fingerprinting based on ¹H-NMR spectroscopy and liquid chromatography for the authentication of herbal products. *Molecules*. 2022; 27(4): 1198. <https://doi.org/10.3390/molecules27041198>
- [19] Yasir B, Alam G. Chemometrics-assisted fingerprinting profiling of extract variation from Pagoda (*Clerodendrum paniculatum* L.) using TLC-Densitometric method. *Egypt J Chem*. 2023; 66(13): 1589-1596. <https://doi.org/10.21608/ejchem.2023.89181.4282>
- [20] Cui C, Xia M, Chen J, Shi B, Peng C, Cai H, Jin L, Hou R. ¹H NMR-based metabolomics combined with chemometrics to detect edible oil adulteration in huajiao (*Zanthoxylum bungeanum* Maxim.). *Food Chem*. 2023; 423: 136305. <https://doi.org/10.1016/j.foodchem.2023.136305>
- [21] Zayed A, Abdelwareth A, Mohamed TA, Fahmy HA, Porzel A, Wessjohann LA, Farag MA. Dissecting coffee seeds metabolome in context of genotype, roasting degree, and blending in the Middle East using NMR and GC/MS techniques. *Food Chem*. 2022; 373: 131452. <https://doi.org/10.1016/j.foodchem.2021.131452>
- [22] Decker C, Krapf R, Kuballa T, Bunzel M. Nontargeted analysis of lipid extracts using ¹H NMR spectroscopy combined with multivariate statistical analysis to discriminate between the animal species of raw and processed meat. *J Agric Food Chem*. 2022; 70(23): 7230-7239. <https://doi.org/10.1021/acs.jafc.2c01871>
- [23] Rebiai A, Seghir BB, Hemmami H, Zeghoud S, Amor IB, Kouadri I, Messaoudi M, Pasdaran A, Caruso G, Sharma S, Atanassova M, Pohl P. Quality assessment of medicinal plants via chemometric exploration of quantitative NMR data: A Review. *Compounds*. 2022; 2(2): 163-181. <https://doi.org/10.3390/compounds2020012>
- [24] Jolliffe I. A 50-year personal journey through time with principal component analysis. *J Multivar Anal*. 2022; 188: 104820. <https://doi.org/10.1016/j.jmva.2021.104820>
- [25] Khan MSI, Islam N, Uddin J, Islam S, Nasir MK. Water quality prediction and classification based on principal component regression and gradient boosting classifier approach. *J King Saud Univ-Com*. 2022; 34(8): 4773-4781. <https://doi.org/10.1016/j.jksuci.2021.06.003>
- [26] Singh MK, Kumar A, Nimmanapalli R, Pandey AK. Proteomics- based milk whey proteome profiling of Indian Jersey cross- breed cows followed by chromosomal mapping. *J Sci Food Agric*. 2023; 102(11): 5634-5640. <https://doi.org/10.1002/jsfa.12640>
- [27] Walls FN, McGarvey DJ. Building a macrosystems ecology framework to identify links between environmental and human health: A random forest modelling approach. *People Nat*. 2023; 5(1): 183-197. <https://doi.org/10.1002/pan3.10427>
- [28] Narvaez-Montoya C, Mahlkecht J, Torres-Martínez JA, Mora A, Bertrand G. Seawater intrusion pattern recognition supported by unsupervised learning: A systematic review and application. *Sci Total Environ*. 2023; 864: 160933. <https://doi.org/10.1016/j.scitotenv.2022.160933>

- [29] Cornea-Cipcigan M, Pamfil D, Sisea CR, Margaoan R. Characterization of Cyclamen genotypes using morphological descriptors and DNA molecular markers in a multivariate analysis. *Front Plant Sci.* 2023; 14: 1100099. <https://doi.org/10.3389/fpls.2023.1100099>
- [30] Das SC, Qais MN, Kuddus MR, Hasan CM. Isolation and characterization of (22E, 24S)-Stigmasta-5, 22, 25-trien-3 β -ol from *Clerodendrum viscosum* Vent. *Asian J Chem.* 2013; 25(11): 6447-6448.
- [31] Akihisa T, Tamura T, Matsumoto T, Kokke WCMC, Ghosh P, Thakur S. (22Z, 24S)-Stigmasta-5, 22, 25-trien-3 β -ol and other novel sterols from *Clerodendrum scandens*: first report of the isolation of a cis- Δ 22-unsaturated sterol from a higher plant. *J Chem Soc Perkin Trans. 1.* 1990; (8): 2213-2218. <https://doi.org/10.1039/P19900002213>
- [32] Oscar NDY, Joel TNS, Ange AANG, Desire S, Brice SNF, Barthelemy N. Chemical constituents of *Clerodendrum splendens* (Lamiaceae) and their antioxidant activities. *J Dis Med Plants.* 2018; 4(5): 120-127. <https://doi.org/10.11648/jjdmp.20180405.11>
- [33] Lin YL, Kuo YH, Chen YL. Two new clerodane-type diterpenoids, clerodinins A and B, from *Clerodendron brachyanthum* Schauer. *Chem Pharm Bull.* 1989; 37(8): 2191-2193. <https://doi.org/10.1248/cpb.37.2191>
- [34] Pandey R, Verma RK, Singh SC, Gupta MM. 4 α -Methyl-24 β -ethyl-5 α -cholesta-14, 25-dien-3 β -ol and 24 β -ethylcholesta-5, 9 (11), 22E-trien-3 β -ol, sterols from *Clerodendrum inerme*. *Phytochemistry.* 2003; 63(4): 415-420. [https://doi.org/10.1016/S0031-9422\(03\)00146-8](https://doi.org/10.1016/S0031-9422(03)00146-8)
- [35] Panthong K, Boonsri S. Chemical constituents from the twigs and stems of *Clerodendrum serratum*. *Burapha Sci J.* 2018; 1330-1344.
- [36] Carballeira NM, Rodriguez J. Two novel phospholipid fatty acids from the Caribbean sponge *Geodia gibberosa*. *Lipids.* 1991; 26(4): 324-326. <https://doi.org/10.1007/BF02537145>
- [37] Barnathan G, Doumenq P, Njinkoué JM, Mirallès J, Debitus C, Lévi C, Komprobst JM. Sponge fatty acids. 3. Occurrence of series of n-7 monoenoic and iso- 5, 9 dienoic long- chain fatty acids in the phospholipids of the marine sponge *Cinachyrella* aff. *schulzei* keller. *Lipids.* 1994; 29(4): 297. <https://doi.org/10.1007/BF02536335>
- [38] Wang D, Zhang J, Li D. Hydrophobic constituents of *Polygonatum odoratum* rhizome from the Qinling mountains and their antiseptic activity. *J Wuhan Bot Res.* 2010; 28(5): 644-647.
- [39] Carballeira NM, Pagán M, Rodríguez AD. Identification and Total synthesis of novel fatty acids from the Caribbean sponge *Calyx podatypa*. *J Nat Prod.* 1998; 61(8): 1049-1052. <https://doi.org/10.1021/np9801413>
- [40] Hegde NP, Hungund BS. Isolation, identification and in vitro biological evaluation of phytochemicals from *Memecylon randerianum*: A medicinal plant endemic to Western Ghats of India. *Nat Prod Res.* 2021; 35(23): 5334-5338. <https://doi.org/10.1080/14786419.2020.1756797>
- [41] Wang P, Guo F, Tan J, Huang C, Wang G, Li Y. A novel C29 sterol from *Clerodendrum cyrtophyllum*. *Chem Nat Compd.* 2012; 48: 594-596. <https://doi.org/10.1007/s10600-012-0320-3>
- [42] Somwong P, Suttisri R. Cytotoxic activity of the chemical constituents of *Clerodendrum indicum* and *Clerodendrum villosum* roots. *J Integr Med.* 2018; 16(1): 57-61. <https://doi.org/10.1016/j.joim.2017.12.004>
- [43] Gleason JG, Ku TW, McCarthy ME, Weichman BM, Holden D, Osborn RR, Zabko-Potapovich B, Berkowitz B, Wasserman MA. 2-nor-leukotriene analogs: antagonists of the airway and vascular smooth muscle effects of leukotriene C4, D4 and E4. *Biochem Biophys Res Commun.* 1983; 117(3): 732-739. [https://doi.org/10.1016/0006-291X\(83\)91658-3](https://doi.org/10.1016/0006-291X(83)91658-3)
- [44] Omoregie GO, Ovuakporie-Uvo O, Idu M. Phyto-composition and antimicrobial activities of the ethanol seed extracts of *Buchholzia coriacea*. *Afr J Pharmacol Therapeut.* 2018; 7(2): 53-58.
- [45] Pakrashi SC, Achari B. Stigmasta-5,22,25-trien-3 β -ol : a new sterol from *Alangium lamarckii* Thw. *Tetrahedron Lett.* 1971; 12(4): 365-368. [https://doi.org/10.1016/S0040-4039\(01\)96443-3](https://doi.org/10.1016/S0040-4039(01)96443-3)
- [46] Ditchou YOG, Kombo CDA, Opono MTGM, Nyasse B. Antioxidant activity of the chemical constituents isolated from the roots of *Albizia ferruginea* (Guill. & Perr.) Benth. (Fabaceae). *J Adv Chem Sci.* 2019; 5(3): 646-651. <https://doi.org/10.30799/jacs.212.19050301>
- [47] Rahim A, Saito Y, Miyake K, Gotodf M, Chen CH, Alam G, Morris-Natschke S, Lee KH, Nakagawa-Goto K. Kleinhospitine E and cycloartane triterpenoids from *Kleinhovia hospita*. *J Nat Prod.* 2018; 81(7): 1619-1627. <https://doi.org/10.1021/acs.jnatprod.8b00211>
- [48] Yasir B, Rahim A, Lallo S, Saito Y, Goto KN, Rohman A, Alam G. Cytotoxicity activity, metabolite profiling, and isolation compound from crude hexane extract of *Cleome ruidospermae*. *Asian Pac J Cancer Prev.* 2023; 24(10): 3345-3352. <https://doi.org/10.31557/APJCP.2023.24.10.3345>
- [49] Houghton P, Fang R, Techatanawat I, Steventon G, Hylands PJ, Lee CC. The sulphorhodamine (SRB) assay and other approaches to testing plant extracts and derived compounds for activities related to reputed anticancer activity. *Methods.* 2007; 42: 377-387. <https://doi.org/10.1016/j.ymeth.2007.01.003>
- [50] Lamkanfi M, Kanneganti TD, Van Damme P, Berghe TV, Vanoverberghe I, Vandekerckhove J, Vandenabeele P, Gevaert K, Nuéñez G. Targeted peptidecentric proteomics reveals caspase-7 as a substrate of the caspase-1 inflammasomes. *Mol Cell Proteomics.* 2008; 7(12): 2350-2363. <https://doi.org/10.1074/mcp.M800132-MCP200>